# Brain structural abnormalities in adult major depressive disorder revealed by voxel- and source-based morphometry: evidence from the REST-meta-MDD Consortium

KangCheng Wang [a*], YuFei Hu [a*], ChaoGan Yan [b,c,d,e], MeiLing Li [f], YanJing Wu [g], Jiang Qiu [h#], XingXing Zhu [i#], the REST-meta-MDD Consortium

[a] School of Psychology, Shandong Normal University, Jinan, Shandong, China

[b] CAS Key Laboratory of Behavioral Science, Institute of Psychology, Beijing, China

[c] Department of Psychology, University of Chinese Academy of Sciences, Beijing, China

[d] Magnetic Resonance Imaging Research Center, Institute of Psychology, Chinese Academy of Sciences, Beijing, China

[e] International Big-Data Center for Depression Research, Institute of Psychology, Chinese Academy of Sciences, Beijing, China

[f] Athinoula A. Martinos Center for Biomedical Imaging, Department of Radiology, Massachusetts General Hospital, Harvard Medical School, Charlestown, MA 02129, USA

[g] Faculty of Foreign Languages, Ningbo University, Ningbo, Zhejiang, China

[h] Faculty of Psychology, Southwest University, Chongqing 400716, China

[i] Institute of Health and Wellbeing, University of Glasgow, Glasgow, UK

Word count, 4608

*These authors contributed equally to this work.

#Corresponding author:
Jiang Qiu
Email: qiuj318@swu.edu.cn
Faculty of Psychology, Southwest University, Chongqing, China
Or
XingXing Zhu
Email: x.zhu.4@research.gla.ac.uk
Institute of Health and Wellbeing, University of Glasgow, Glasgow, UK

# Abstract

## Background

Neuroimaging studies on major depressive disorder (MDD) have identified an extensive range of brain structural abnormalities, but the exact neural mechanisms associated with MDD remain elusive. Most previous studies were performed with voxel‐or surface‐based morphometry which were univariate methods without considering spatial information across voxels/vertices.

## Methods

Brain morphology was investigated using voxel‐based morphometry (VBM) and source‐based morphometry (SBM) in 1082 MDD patients and 990 healthy controls (HC) from the REST-meta-MDD Consortium. We first examined group differences in regional grey matter volumes and structural covariance networks between patients and HCs. We then compared first episode, drug-naïve (FEDN) patients, and recurrent patients. Additionally, we assessed the effects of symptom severity and illness duration on brain alterations.

## Results

VBM showed decreased grey matter volume in various regions in MDD patients including the superior temporal cortex, anterior and middle cingulate cortex, inferior frontal cortex, and precuneus. SBM returned differences only in the prefrontal network. Comparisons between FEDN and recurrent MDD patients showed no significant differences by VBM, but SBM showed greater decreases in prefrontal, basal ganglia, visual and cerebellar networks in the recurrent group. Moreover, depression severity was associated with volumes in the inferior frontal gyrus and precuneus, as well as the prefrontal network.

## Conclusions

Simultaneous application of VBM and SBM methods revealed brain alterations in MDD patients and specified differences between recurrent and FEDN patients, which tentatively provide an effective multivariate method to identify potential neurobiological markers for depression.



## Keywords

major depressive disorder; voxel‐based morphometry; source‐based morphometry; brain structure; structural covariance network

## Introduction

Major depressive disorder (MDD) is a common and debilitating psychiatric disorder. It is among the leading causes of disability worldwide, with a lifetime prevalence of >16% (Kessler et al., 2007). The pathophysiology of major depression remains elusive despite intensive efforts made to identify the neurobiological mechanisms. Over the last decades, structural magnetic resonance imaging (MRI) has been widely used in investigating morphological brain differences in MDD. The two largest meta-analyses based on cohorts worldwide in the ENIGMA (Enhancing NeuroImaging Genetics through Meta-Analysis) MDD Working Group (Schmaal et al., 2020) have reported specific abnormalities, such as thinner orbitofrontal cortex and smaller hippocampal volumes (Schmaal et al., 2017; Schmaal et al., 2016). Recent evidence also suggests abnormal grey matter volume and cortical thickness in various brain regions (Ancelin et al., 2019; Binnewies et al., 2021; Kandilarova, Stoyanov, Sirakov, Maes, & Specht, 2019; Q. Li et al., 2020). To date, structural abnormalities in MDD have not been reported consistently across studies. Moreover, most previous studies were performed with either voxel‐or surface‐based morphometry (Enneking, Leehr, Dannlowski, & Redlich, 2020; Kocsis et al., 2021; Q. Li et al., 2020; Serra-Blasco et al., 2021), both of which were univariate methods fail to consider spatial information (covariation) across voxels/vertices.

MDD has been investigated as a potentially brain network-based disorder (Gong & He, 2015; B. J. Li et al., 2018; Menon, 2011). Abnormalities in the structural covariation were reported in previous studies (Han et al., 2020; Wu et al., 2017) that calculated the correlation between grey matter (GM) volume within predefined regions of interest. However, this approach did not fully capture patterns of structural covariation. Recently, the source-based morphometry (SBM) has provided a novel approach to examine whole-brain structural covariance networks. It is a multivariate, data-driven approach that applies independent component analysis (ICA) to segmented GM images and extracts clusters of GM voxels covarying across participants as structural networks (Xu, Groth, Pearlson, Schretlen, & Calhoun, 2009). SBM could identify covarying networks across distinct voxels, rather than focusing on each voxel separately. For brain imaging, SBM provides two major advantages: (1) it does not need to predefine regions of interest and (2) it separates artifacts and real brain change with high precision (Gupta, Turner, & Calhoun, 2019). Prior studies suggested that structural covariance patterns of brain regions are highly related with functional networks, demonstrating significant spatial overlaps (Spreng & Turner, 2013; Zielinski, Gennatas, Zhou, & Seeley, 2010). Recently, researchers highlighted that structural networks were enriched with brain local molecular and cellular metadata, and that it is connected with more nuanced representations of functional networks and properties (Suarez, Markello, Betzel, & Misic, 2020). Using SBM, the structural networks have been widely identified in cognitive and affective aspects, such as intelligence (Yoon et al., 2017) and suicidal behavior (Harenski, Harenski, Calhoun, & Kiehl, 2020), as well as psychiatric disorders including autism (Pappaianni et al., 2018), bipolar disorder (Singh, Arya, Agarwal, Shree, & Kumar, 2021), schizophrenia (Gupta et al., 2015; Xu et al., 2009), and MDD (Depping et al., 2016; Watanabe et al., 2020; Yang et

al., 2021). These findings showcased advantages of SBM in understanding brain structural covariations in both healthy and psychiatric populations.

Although previous studies have investigated the structural covariance networks in MDD (Depping et al., 2016; Kakeda et al., 2020; Nguyen et al., 2020; Okamoto et al., 2020; Watanabe et al., 2020; Wolf et al., 2016; Yang et al., 2021), the exact pattern of abnormalities in structural covariance networks remains unclear. While an earlier study found decreased volume in the fronto-striatal network, cingulate, and lateral prefrontal regions (Depping et al., 2016), extensive abnormalities in the salience network, medial temporal lobe network, default mode network, and central executive network have also been reported (J. Li et al., 2021; Watanabe et al., 2020). Such inconsistency might be due to the clinical heterogeneity in MDD patients and/or small sample size. Several studies were conducted with around 20 MDD patients (Depping et al., 2016; Okamoto et al., 2020; Wolf et al., 2016), and the largest study to date examined only 145 MDD patients (Yang et al., 2021). Small sample size limited the statistical power to detect subtle differences in brain structural abnormalities. Furthermore, previous studies were conducted with first-episode and drug-naïve (FEDN) MDD patients (Kakeda et al., 2020; Nguyen et al., 2020; Watanabe et al., 2020) or those with recurrent episodes (Depping et al., 2016). However, the differences in structural networks between first-episode and recurrent patients remain poorly examined, given that inconsistent patterns of structural abnormalities have been reported in the two ENIGMA studies (Schmaal et al., 2017; Schmaal et al., 2016). In addition, the relationship between whole-brain structural networks and clinical symptoms in MDD has not been well established. To our knowledge, only one study has investigated this issue and reported a negative correlation between the “cingulate network” and the Hamilton Depression Rating Scale (HAMD) total score (Depping et al., 2016). Taken together, these findings highlighted the necessity to explore whole brain structural covariance networks in MDD with a focus on the relationship between recurrence status and clinical symptoms based on larger well-powered samples.

In this study, we aimed to investigate brain structural abnormalities in regional GM volume and structural covariance networks associated with MDD within a large, multi-site sample drawn from the REST-meta-MDD Project in China (C. G. Yan et al., 2019). VBM was applied to acquire regional GM volumes and a novel SBM approach was carried out to obtain structural covariance networks based on GM images. We first compared regional GM volume and structural covariance networks between 1082 MDD patients and 990 HCs and then examined effects of clinical characteristics (i.e., single vs recurrent episodes, symptom severity) on potential brain abnormalities in MDD patients.

# Methods

## Participants

A total of 1082 patients with MDD and 990 HCs from 20 sites of the REST-meta-MDD consortium were recruited for this study (C. G. Yan et al., 2019). All study sites obtained approval from their local institutional review boards and ethics committees. All participants provided written informed consent before participation. As reported previously, participants were identified as “patients” if he/she had a past or current MDD episode according to the DSM-5 or ICD-10 (C. G. Yan et al., 2019). All participants in the HC group did not have a prior or current episode of any psychiatric disorder based on ICD-10 or DSM-5 at the time of investigation. We excluded 308 participants for the following reasons: 1) the information on gender, age, or education was unavailable; 2) poor imaging quality or bad spatial normalization (via visual inspection); 3) younger than 18 years old; 4) from a site with a sample size of patients or controls smaller than 10; and 5) sample replication (site S4 was duplicated from site S14). Severity of depression and anxiety in patients was assessed using the 17-item Hamilton Depression Rating Scale (HAMD) and the Hamilton Anxiety Rating Scale (HAMA) separately in 19 and 10 sites. Finally, we examined 874 patients from 17 sites with information on duration of illness, 1006 patients from 19 sites with HAMD scores, and 637 patients from 10 sites with HAMA scores. According to the episode and medical information from 637 patients of 6 sites, 430 patients were first episode and drug-naïve (FEDN MDD group) and the rest 207 had experienced more than one episode of MDD (i.e., the recurrent group). See Table 1 for detailed information of all patients, HCs, FEDN, and recurrent MDD groups. The demographic and clinical information for participants in each site was summarized in Table S1.

----------**INSERT TABLE 1 HERE**----------

## Data Acquisition

MRI scans were acquired at each local site. Data acquisition parameters for T1 weighted structural images including the scanner, time repetition, and voxel size were replicated as in a prior study (C. G. Yan et al., 2019).

## Voxel-based Morphometry Processing

Structural MRI data for all participants were preprocessed at each site, using the same DPARSF protocol (Chao Gan. Yan & Zang, 2010). In brief, a fully automatic technique for the computational analysis of differences in regional brain volume throughout the brain was conducted using the SPM methods (Statistical Parametric Mapping; Institute of Neurology, London, UK). The T1 images in native space were segmented into GM and

white matter images and then modulated and spatially normalized using the Diffeomorphic Anatomical Registration Through Exponential Lie Algebra (DARTEL) toolbox (Ashburner, 2007). To preserve the GM volume within each voxel, the processed images were modulated using the Jacobean determinants derived from the spatial normalization by DARTEL. The shared modulated GM images were then smoothed using an 8 mm full-width at half-maximum Gaussian kernel.

### Source-based Morphometry Processing

With the preprocessed GM images, we carried out the SBM processing using the GIFT toolbox (https://trendscenter.org/software). The number of independent components (ICs, i.e. GM structural networks) was 17 (Kakeda et al., 2020). We performed principal component analysis using a neural network algorithm (Infomax), which minimized mutual information of the network outputs in order to identify naturally grouping and maximally independent sources (Bell & Sejnowski, 1995). This process was repeated 20 times in ICASSO (http://research.ics.aalto.fi/ica/icasso/) to ensure the consistency and reliability of the resulting components. Of the 17 ICs, four were judged as artifacts based on the criteria defined by Xu et al. (2009). Recent studies suggested that cerebellar circuits not only consisted of motor related networks, but also the networks related to cognition, emotion, and depression (D'Mello, Gabrieli, & Nee, 2020; Pierce & Peron, 2020; Sokolov, Miall, & Ivry, 2017). Thus, two ICs that mainly included cerebellar networks were also subject to subsequent analyses. As a result, a total number of 13 independent components were examined (see Supplementary Figure S1).

In the calculation for ICs, all preprocessed images were arrayed into a 2D matrix, with each row representing a participant, and each column indicating a voxel. This matrix was then decomposed into 2 matrices by the ICA. The first matrix (mixing matrix, size = 2072 x 13) consisted of one participant per row and an IC per column. It involved “loading coefficients” demonstrating how each structural component contributed to the GM characteristics of 2072 subjects. The loading coefficients were then transformed into z-scores before analyses. The second matrix (source matrix), which specified the relationship between the ICs and the voxels, was used for the visualization of components. To produce brain maps, the source matrix was reshaped back into a three-dimensional brain image and scaled to unit standard deviations (Z maps).

## Statistical analyses

### Voxel-based Morphometry Analysis

The VBM analyses were performed using the SPM8. Whole-brain GM differences between the MDD group and HCs were assessed using the two-sample t-test. Age, gender, education, and the scanning site were included as covariates of no interest. This

analysis yielded statistical parametric maps based on a voxel-level threshold of $p < 0.001$. The cluster-level family wise error (FWE) correction was applied for multiple comparisons ($p < 0.05$).

**Source-based Morphometry Analysis**

SBM analyses were performed using the SBM statistical tool and Matlab (2019b). The loading coefficients were compared between the MDD group and HCs, using two-sample t-tests in SBM. Age, gender, education, and sites were included as covariates. Results were corrected with the Bonferroni method at $p < 0.05$ (i.e. threshold was $p < 0.05/13$, 13 means the number of ICs).

In addition, a validation analysis with 30 ICs was conducted as suggested in previous studies (Castro et al., 2016; Harenski et al., 2020). Nine components contained sharp edges near the boundary of the brain or appeared primarily in regions that do not contain GM. Thus, we repeated above analyses for the rest 21 ICs.

**Influence of Recurrence Status**

To examine the influence of recurrence status on GM differences, we compared regional GM volume and structural covariance networks (loading coefficients) between FEDN MDD and HC participants, recurrent MDD and HC participants, and FEDN MDD and recurrent MDD participants. Two-sample t-tests were performed with age, gender, education, and sites included as covariates. Bonferroni correction at $p < 0.05$ was applied to VBM and SBM results separately.

**Association with Clinical Characteristics**

Finally, to explore the association between clinical characteristics and structural abnormalities in MDD patients, we performed partial correlation analyses for symptom severity (HAMD, HAMA) and illness duration. Age, gender, education, and sites were included as covariates. Results were corrected with the Bonferroni correction method at $p < 0.05$ (i.e. $p < 0.05/n$, n represents the number of significant brain regions or networks) for VBM and SBM separately.

# Results

## Demographic Results

Demographic information including age, gender, and education for MDD patients (n = 1082) and HCs (n = 990) were shown in Table 1 and Table S1. The two groups matched on both gender ($x^2 = 1.48$, $p = 0.223$) and age ($t = -1.72$, $p = 0.085$). The HC group received significantly more education as compared to MDD group (MDD group = 11.63 ± 3.71, HC group = 13.25 ± 3.73; $t = 1.11$, $p < 0.001$). On average, MDD patients had a 38-month course of disease and a severe level of symptoms (HAMD = 20.75 ± 7.48).

The FEDN and recurrent MDD groups matched on gender, age, and education (Table 1). The recurrent MDD group had significantly longer illness duration as compared to the FEDN MDD group (FEDN MDD group = 21.60 ± 37.69, recurrent MDD group = 94.67 ± 87.04; t = -14.78, p < 0.001). However, as compared to the recurrent MDD group, FEDN MDD patients scored higher in HAMD (FEDN MDD group = 21.44 ± 5.87, recurrent MDD group = 19.10 ± 7.85; t = 4.20, p < 0.001) and HAMA (FEDN MDD group = 21.52 ± 8.75, recurrent MDD group = 17.57 ± 8.65; t = 4.39, p < 0.001).

## Voxel-based morphometry

### Group Differences in Grey Matter Regional Volumes

As compared to HCs, MDD patients showed reduced GM volume in bilateral superior temporal cortices (left, MNI x/y/z = -46.5/10.5/-9, cluster size = 293, t = -6.90; right, MNI x/y/z = 49.5/13.5/-4.5, cluster size = 141, t = -7.02), dorsal anterior cingulate cortex (MNI x/y/z = 0/9/24, cluster size = 435, t = -6.25), right middle cingulate cortex (MNI x/y/z = 13.5/-21/36, cluster size = 169, t = -6.28), right inferior frontal cortex (MNI x/y/z = 42/13.5/21, cluster size = 134, t = -6.85), and precuneus (MNI x/y/z = 21/-61.5/42, cluster size = 100, t = -5.90). Brain regions and locations of these effects were shown in Figure 1 and Table 2. No increases of GM volumes were found in MDD patients.

----------**INSERT FIGURE 1 HERE**----------

----------**INSERT TABLE 2 HERE**----------

### Influence of Recurrence Status on Grey Matter Regional Volumes

As compared to HCs (n = 990), neither FEDN (n = 430) nor recurrent MDD (n = 207) groups showed any significant difference in GM regional volume (FWE correction). When comparing FEDN MDD patients with recurrent MDD patients, no significant difference was observed either. Nonetheless, at an uncorrected level of $p < 0.05$, recurrent and FEDN patients showed similar GM atrophy (see Figure S2).

### Association of Grey Matter Regional Volumes with Symptom Severity and Illness Duration

In the MDD patients, partial correlation analyses revealed that increased depression severity (HAMD, n = 1066) was negatively correlated with GM volume in the right inferior frontal gyrus ($r = -0.10$, $p_{bonferroni} < 0.05$) and precuneus ($r = -0.12$, $p_{bonferroni} < 0.05$). There was no correlation between regional GM volumes and anxiety severity (HAMA, n = 637), or illness duration (n = 874).

## Source-based morphometry

### Group Differences in Grey Matter Networks

Significant between-group difference was observed in the “prefrontal network” of the ICs (Figure 2, Table 3). Regions of the prefrontal network included the middle, superior, inferior frontal gyri, and precentral gyrus (Table 4). The average z-score for this component in MDD patients (-0.08 ± 0.98) was significantly lower than that of HCs (0.08 ± 1.02). In the validation analyses based on 30 ICs, the difference in prefrontal network was also significant different between MDD patients (-0.074 ± 0.969) and HCs (0.031 ± 1.013). In addition, the location of prefrontal network in this comparison, which included the middle, superior, and medial frontal cortices (Figure S3), was similar to that emerged from the main analyses.

----------**INSERT FIGURE 2 HERE**----------

----------**INSERT TABLE 3 HERE**----------

### Influence of Recurrence Status on Grey Matter Networks

As compared to HCs (n = 990), the FEDN MDD group (n = 430) showed higher mean z-scores in the cerebellar A network (FEDN MDD = 0.21 ± 0.66, HCs = 0.01 ± 1.03; Figure 2; Table 3) and lower mean z-scores in the superior temporal network (FEDN MDD = -0.20 ± 0.96, HCs = 0.04 ± 1.03). Locations of these structural covariance networks were shown in the Table 4.

In addition, as compared to HCs (n = 990), the recurrent MDD group (n = 207) showed decreased z-scores in two cerebellar networks (network A, recurrent MDD: -0.22 ± 0.99, HCs: 0.01 ± 1.03; network B, recurrent MDD: -0.21 ± 1.05, HCs: 0.01 ± 1.02; Table 3), basal ganglia network (recurrent MDD: -0.88 ± 1.17; HCs: 0.003 ± 1.00), temporal network (recurrent MDD: -0.33 ± 0.95; HCs: 0.04 ± 1.03), prefrontal network (recurrent MDD: -0.17 ± 1.10; HCs: 0.08 ± 1.02), and visual network (recurrent MDD: -0.27 ± 0.94; HCs: -0.014 ± 1.00), and increased z-scores in parietal network (recurrent MDD: 0.29 ± 0.95; HCs: 0.04 ± 1.02). See figure 2 and Table 4 for the locations of these structural covariance networks.

The recurrent MDD group had significantly lower z-scores than the FEDN MDD group in five networks (see Table 3) including the basal ganglia network (FEDN: -0.07 ± 0.75; recurrent: -0.88 ± 1.17), visual network (FEDN: 0.08 ± 0.98; recurrent: -0.27 ± 0.94), and two cerebellar networks (cerebellar network A: 0.21 ± 0.66 and -0.22 ± 0.99; cerebellar network B: 0.14 ± 0.93 and -0.21 ± 1.05). In the prefrontal network, the z-scores in recurrent MDD patients (FEDN: 0.08 ± 0.99; recurrent: -0.17 ± 1.10, $p_{bonferroni} = 0.06$) were modestly lower than those in FEDN MDD patients. Validation analyses showed similar results (Figure S3).

----------**INSERT TABLE 4 HERE**----------

### Association of Grey Matter Source Volumes with Symptom Severity and Illness Duration

Partial correlation analyses showed that in the MDD group, increased depression severity (HAMD, n = 1066) was negatively correlated with z scores in the prefrontal network ($r = -0.08$, $p_{bonferroni} < 0.05$). There was no correlation between the prefrontal network and either anxiety severity or illness duration. Given that several structural networks were different between the FEDN and recurrent MDD patients, we also investigated potential correlations in the FEDN MDD group and in the recurrent MDD patients respectively. Results showed no correlation between GM networks and either symptom severity or illness duration in FEDN and recurrent MDD patients.

## Discussion

To our best knowledge, this is the largest study to investigate structural covariance networks in MDD combining both VBM and SBM approaches in searching for brain structural biomarkers for MDD. VBM analyses found reduced GM volume in superior temporal cortices, cingulate cortices, inferior frontal cortex, and precuneus in MDD patients as compared to HCs. SBM analyses showed lower z-scores in the prefrontal network in MDD patients as compared to HCs. In addition, we identified extensive differences in structural covariance networks between FEDN and recurrent MDD patients. Furthermore, correlations with depression severity were also observed for specific brain regions and the prefrontal network. Our identification of abnormalities in the GM volume and structural covariance networks heightened the understanding of structural mechanisms in patients with MDD and the damages of recurrence on depressed brain structure.

The VBM findings showed decreased regional GM volume in the bilateral superior temporal cortices, dorsal anterior cingulate cortex, right middle cingulate cortex, right inferior frontal cortex, and precuneus in MDD patients. These findings are consistent with previous structural research on GM volume, cortical thickness, and surface area in depression (Kandilarova et al., 2019; Schmaal et al., 2020; Serra-Blasco et al., 2021; Shen et al., 2021). Prior studies suggested that superior temporal regions responsive to sad stimuli, and its activation was lower in MDD patients (Fitzgerald, Laird, Maller, & Daskalakis, 2008). Dorsal anterior cingulate cortex was mainly associated with cognitive processes and evaluation of reward values (Bush et al., 2002; Jahn, Nee, Alexander, & Brown, 2016). Damage to the right inferior frontal gyrus impairs the performance on behavioral inhibition (Aron, Robbins, & Poldrack, 2014; Rolls et al., 2020). Precuneus is a core region of the default mode network, and abnormalities in this region have been associated with low self-esteem and high rumination in depression (Cheng et al., 2018). Our results also showed that severity of depression symptoms was associated with

regional GM volume in the right inferior frontal gyrus and precuneus, which further suggest that these structural abnormalities were associated with various domains of depression.

Although VBM showed structural abnormalities related to MDD, it failed to detect abnormal GM clusters in the comparisons between the FEDN group and the recurrent MDD group. Uncorrected brain maps demonstrated that FEDN and recurrent patients had a similar trend and distribution of GM atrophy. These results suggested that FEDN and recurrent patients had similar abnormalities in local brain regions. To distinguish the differences related to episodes, a network perspective would be needed.

The SBM analyses identified thirteen structural covariance networks in total and significant differences were found in seven of them, especially the prefrontal network (Table 3). The prefrontal network effect was significant in MDD group vs. HCs, recurrent MDD vs. HCs and recurrent MDD vs. FEDN MDD group in this large, multi-site sample. This network encompassed regions mainly in the prefrontal cortex (Table 4), which has been associated with many processes such as cognitive control (Miller, 2000) and emotional regulation (Dixon, Thiruchselvam, Todd, & Christoff, 2017). A previous study reported abnormal prefrontal networks in FEDN patients as compared to healthy controls (Kakeda et al., 2020). In addition, the prefrontal network was negatively associated with levels of severity of depression symptoms. Therefore, our findings suggest that depression was associated with low structural covarying in prefrontal network. The prefrontal regions might not work together cohesively in depressive patients and thus they might encounter problems in emotion regulation and attention to negative stimuli (Disner, Beevers, Haigh, & Beck, 2011; L. Wang et al., 2008; Zhou et al., 2020).

Other structural covariance networks identified in FEDN MDD vs HCs or recurrent MDD vs HCs included basal ganglia network, temporal network, parietal network, visual network and two cerebellar control networks. The basal ganglia network has been implicated in processing rewards (Haber, 2008; Schultz, Tremblay, & Hollerman, 2000), and has been a critical neural marker for antidepressant and neuromodulating intervention in MDD and other psychiatric disorders (Bewernick et al., 2010; Schneier et al., 2018). The temporal network has been known to engage in emotional memory (Murty, Ritchey, Adcock, & LaBar, 2010); the parietal network is thought to play a role in attention control (Rohr et al., 2017); the visual network has been associated with visual processing biases in MDD (Desseilles et al., 2009). Both structural and functional abnormalities in these networks have been constantly observed in patients with MDD (Gong & He, 2015; T. Wang et al., 2016). By contrast, the cerebellar control does not have a well-established role in current literature of depression, although abnormal volume and function in the cerebellum have been reported in MDD (Bogoian, King, Turner, Semmel, & Dotson, 2020; Kaiser, Andrews-Hanna, Wager, & Pizzagalli, 2015). Structural abnormalities may contribute to decreases in brain functioning levels in affected regions (Paquola, Bennett, & Lagopoulos, 2018; Suarez et al., 2020). The abnormalities in structural covariance networks supported the idea that MDD might be a brain network-based disorder. A recent

review study supported the more reliable biomarkers of psychiatric disorders with a network viewpoint (Sullivan, Olsen, & Widge, 2021). Scangos et al. (2021) implemented the networks perspective with deep based stimulation, with focal stimulation identifying individual symptom-specific biomarker and a treatment region stimulating for symptoms improvement. As a result, network mapping and related biomarker stimulation reduced depressive symptoms and improved depression status sustainably. Taken together, brain structural networks might be valuable as potential intervention and treatment targets, especially for those that have been associated with cognition and emotion processes in depression.

It is not surprising that there is no direct overlap between the results of VBM and SBM. As explained by Xu et al. (2009), SBM differs from VBM in utilizing the interrelationship among voxels, spatially filtering artificial sources, capturing covariation of specific sources and minimizing the number of comparisons. Previous studies comparing VBM with SBM demonstrated that SBM might be more sensitive in detecting structural abnormalities (Harenski et al., 2020; Pappaianni et al., 2018; Xu et al., 2009), while opposite findings were also reported (Kunst et al., 2019). When compared to surface-based morphometry (e.g., cortical thickness), results were also inconsistent (Kunst et al., 2019; Pappaianni et al., 2018). In this study, the SBM method revealed effects that were not detected by VBM in basal ganglia, occipital lobe, and the cerebellar in the comparisons between FEDN and recurrent MDD patients, indicating that SBM might be more sensitive than VBM to morphometry abnormalities. Our results are consistent with Xu et al. (2009), as SBM could incorporate additional information about the grouping of the regions within several distinct, anatomically consistent sources. Future studies could apply SBM to identify biomarkers of structural covariance networks in MDD and other neurobehavioral disorders.

Another interesting finding was that recurrent MDD patients, as compared to the FEDN patients, showed significantly greater abnormalities in the prefrontal network, basal ganglia network, visual network, and two cerebellar control networks. In addition, the difference in prefrontal network observed in the comparison between MDD group and HCs was driven by recurrent MDD participants. These results corresponded to brain structural and functional differences between first-episode and recurrent patients that were reported in previous literature (Schmaal et al., 2017; Schmaal et al., 2016; C. G. Yan et al., 2019). Previous studies suggested that MDD had a high rate of recurrence, with approximately 50%-60% of patients suffering recurrence after an initial episode (Burcusa & Iacono, 2007; Nobbelin, Bogren, Mattisson, & Bradvik, 2018). Our identification of abnormal structural covariance networks in recurrent MDD is a significant contribution to understanding recurrent MDD. These results suggest that treatment of recurrent MDD patients may need to focus more on brain networks.

The cross-sectional design of the present study prevents it from determining whether the abnormalities observed existed before or after MDD. Future longitudinal studies are needed to investigate the developmental trajectory of regional volumes and structural

covariance networks, and to associate potential differences to symptom profiles and treatment responses. The heterogeneity in MDD patients who were recruited across 20 sites is also expected to be considerable. Whole-group analyses were limited by varied recurrence status, medication status, illness duration, and symptoms severity, which were tested for in the analyses. As we found, delineating differences in first episode/recurrent and other associations would have revealed more neurobiologically characteristics and clinically meaningful findings. Finally, as previous studies showed, patterns of brain abnormalities and symptom profiles in adults and adolescents with MDD might be different (Rice et al., 2019; Schmaal et al., 2017). The data collected in this study does not allow a reliable investigation of brain morphometry in adolescents, because of the sample size and heterogeneity of sample sources, with 47 adolescent MDD patients from seven sites and 19 normal adolescents from two of those sites. Differences in structural covariance networks between adolescent MDD patients, adult MDD patients, and HCs require further investigation.

**Conclusion**

Our findings suggest that MDD patients exhibit abnormalities in both selected brain regions and certain structural covariance networks. VBM showed more scattered brain regions as compared to SBM when comparing between the whole MDD group and HCs, but SBM found more robust and widespread abnormalities in the recurrent MDD group as compared to FEDN MDD. Analysis of clinical characteristics suggests that diverse patient populations might present significant confounders in neuroimaging findings in major depression. Taken together, the VBM and SBM are expected to reveal different profiles of structural abnormalities related to MDD. Future longitudinal studies are needed to examine brain changes in regions/networks highlighted in the present study, and to establish links between differences in symptom profiles and treatment responses in MDD.

## Financial support

This research was supported by the National Natural Science Foundation of China (32000760) to KW, China Postdoctoral Science Foundation Funded Project to KW (2019M662433), Postdoctoral Innovation Project (239735) in Shandong Province to KW, the National Social Science Foundation of China (21AYY014) and the Fundamental Research Funds for the Provincial Universities of Zhejiang to YW.

## Conflicts of Interest

The authors declare no competing financial interests.

## Acknowledgements

The REST-meta-MDD consortium was initiated and established by Dr. Chaogan Yan, who came from the Institute of Psychology, Chinese Academy of Sciences. This consortium aimed to address limited statistical power and analytic heterogeneity of major depressive

disorder. For this purpose, twenty-five research groups from 17 hospitals in China formed the REST-meta-MDD consortium and agreed to share final resting state fMRI indices and the structural data of patients with depression and matched normal controls. Detailed information can be found in http://rfmri.org/REST-meta-MDD. Researchers in the REST-meta-MDD consortium include Chao-Gan Yan, Xiao Chen, Le Li, Francisco Xavier Castellanos, Tong-Jian Bai, Qi-Jing Bo, Jun Cao, Guan-Mao Chen, Ning-Xuan Chen, Wei Chen, Chang Cheng, Yu-Qi Cheng, Xi-Long Cui, Jia Duan, Yi-Ru Fang, Qi-Yong Gong, Wen-Bin Guo, Zheng-Hua Hou, Lan Hu, Li Kuang, Feng Li, Kai-Ming Li, Tao Li, Yan-Song Liu, Zhe-Ning Liu, Yi-Cheng Long, Qing-Hua Luo, Hua-Qing Meng, Dai-Hui Peng, Hai-Tang Qiu, Jiang Qiu, Yue-Di Shen, Yu-Shu Shi, Chuan-Yue Wang, Fei Wang, Kai Wang, Li Wang, Xiang Wang, Ying Wang, Xiao-Ping Wu, Xin-Ran Wu, Chun-Ming Xie, Guang-Rong Xie, Hai-Yan Xie, Peng Xie, Xiu-Feng Xu, Hong Yang, Jian Yang, Jia-Shu Yao, Shu-Qiao Yao, Ying-Ying Yin, Yong-Gui Yuan, Ai-Xia Zhang, Hong Zhang, Ke-Rang Zhang, Lei Zhang, Zhi-Jun Zhang, Ru-Bai Zhou, Yi-Ting Zhou, Jun-Juan Zhu, Chao-Jie Zou, Tian-Mei Si, Xi-Nian Zuo, Jing-Ping Zhao, and Yu-Feng Zang. We gratefully acknowledge all of them and all participants.

## REFERENCE

Ancelin, M. L., Carriere, I., Artero, S., Maller, J., Meslin, C., Ritchie, K., . . . Chaudieu, I. (2019). Lifetime major depression and grey-matter volume. *Journal of Psychiatry & Neuroscience, 44*(1), 45-53. doi:10.1503/jpn.180026

Aron, A. R., Robbins, T. W., & Poldrack, R. A. (2014). Inhibition and the right inferior frontal cortex: one decade on. *Trends in Cognitive Sciences, 18*(4), 177-185. doi:10.1016/j.tics.2013.12.003

Ashburner, J. (2007). A fast diffeomorphic image registration algorithm. *Neuroimage, 38*(1), 95-113. doi:10.1016/j.neuroimage.2007.07.007

Bell, A. J., & Sejnowski, T. J. (1995). An information-maximization approach to blind separation and blind deconvolution. *Neural Computation, 7*(6), 1129-1159. doi:10.1162/neco.1995.7.6.1129

Bewernick, B. H., Hurlemann, R., Matusch, A., Kayser, S., Grubert, C., Hadrysiewicz, B., . . . Schlaepfer, T. E. (2010). Nucleus accumbens deep brain stimulation decreases ratings of depression and anxiety in treatment-resistant depression. *Biological Psychiatry, 67*(2), 110-116. doi:10.1016/j.biopsych.2009.09.013

Binnewies, J., Nawijn, L., van Tol, M. J., van der Wee, N. J. A., Veltman, D. J., & Penninx, B. (2021). Associations between depression, lifestyle and brain structure: A longitudinal MRI study. *Neuroimage, 231*, 117834. doi:10.1016/j.neuroimage.2021.117834

Bogoian, H. R., King, T. Z., Turner, J. A., Semmel, E. S., & Dotson, V. M. (2020). Linking depressive symptom dimensions to cerebellar subregion volumes in later life. *Translational Psychiatry, 10*(1), 201. doi:10.1038/s41398-020-00883-6

Burcusa, S. L., & Iacono, W. G. (2007). Risk for recurrence in depression. *Clinical Psychology Review, 27*(8), 959-985. doi:10.1016/j.cpr.2007.02.005

Bush, G., Vogt, B. A., Holmes, J., Dale, A. M., Greve, D., Jenike, M. A., & Rosen, B. R. (2002). Dorsal anterior cingulate cortex: a role in reward-based decision making. *Proceedings of the National Academy of Sciences of the United States of America, 99*(1), 523-528. doi:10.1073/pnas.012470999

Castro, E., Hjelm, R. D., Plis, S. M., Dinh, L., Turner, J. A., & Calhoun, V. D. (2016). Deep Independence Network Analysis of Structural Brain Imaging: Application to Schizophrenia. *IEEE Transactions on Medical Imaging, 35*(7), 1729-1740. doi:10.1109/TMI.2016.2527717

Cheng, W., Rolls, E. T., Qiu, J., Yang, D. Y., Ruan, H. T., Wei, D. T., . . . Feng, J. F. (2018). Functional Connectivity of the Precuneus in Unmedicated Patients With Depression. *Biological Psychiatry: Cognitive Neuroscience and Neuroimaging, 3*(12), 1040-1049. doi:10.1016/j.bpsc.2018.07.008

D'Mello, A. M., Gabrieli, J. D. E., & Nee, D. E. (2020). Evidence for Hierarchical Cognitive Control in the Human Cerebellum. *Current Biology, 30*(10), 1881-1892. doi:10.1016/j.cub.2020.03.028

Depping, M. S., Wolf, N. D., Vasic, N., Sambataro, F., Thomann, P. A., & Wolf, R. C. (2016). Common and distinct structural network abnormalities in major depressive disorder and borderline personality disorder. *Progress in Neuro-Psychopharmacology and Biological Psychiatry, 65*, 127-133. doi:10.1016/j.pnpbp.2015.09.007

Desseilles, M., Balteau, E., Sterpenich, V., Dang-Vu, T. T., Darsaud, A., Vandewalle, G., . . . Schwartz, S. (2009). Abnormal neural filtering of irrelevant visual information in depression. *Journal of Neuroscience, 29*(5), 1395-1403. doi:10.1523/JNEUROSCI.3341-08.2009

Disner, S. G., Beevers, C. G., Haigh, E. A., & Beck, A. T. (2011). Neural mechanisms of the cognitive model of depression. *Nat Rev Neurosci, 12*(8), 467-477. doi:10.1038/nrn3027

Dixon, M. L., Thiruchselvam, R., Todd, R., & Christoff, K. (2017). Emotion and the prefrontal cortex: An integrative review. *Psychological Bullutin, 143*(10), 1033-1081. doi:10.1037/bul0000096

Enneking, V., Leehr, E. J., Dannlowski, U., & Redlich, R. (2020). Brain structural effects of treatments for depression and biomarkers of response: a systematic review of neuroimaging studies. *Psychological Medicine, 50*(2), 187-209. doi:10.1017/S0033291719003660

Fitzgerald, P. B., Laird, A. R., Maller, J., & Daskalakis, Z. J. (2008). A meta-analytic study of changes in brain activation in depression. *Human Brain Mapping, 29*(6), 683-695. doi:10.1002/hbm.20426

Gong, Q. Y., & He, Y. (2015). Depression, neuroimaging and connectomics: a selective overview. *Biological Psychiatry, 77*(3), 223-235. doi:10.1016/j.biopsych.2014.08.009

Gupta, C. N., Calhoun, V. D., Rachakonda, S., Chen, J., Patel, V., Liu, J., . . . Turner, J. A. (2015). Patterns of Gray Matter Abnormalities in Schizophrenia Based on an International Mega-analysis. *Schizophrenia Bulletin, 41*(5), 1133-1142. doi:10.1093/schbul/sbu177

Gupta, C. N., Turner, J. A., & Calhoun, V. D. (2019). Source-based morphometry: a decade of covarying structural brain patterns. *Brain Structure and Function, 224*(9), 3031-3044. doi:10.1007/s00429-019-01969-8

Haber, S. (2008). Parallel and integrative processing through the Basal Ganglia reward circuit: lessons from addiction. *Biological Psychiatry, 64*(3), 173-174.

doi:10.1016/j.biopsych.2008.05.033

Han, S., Cui, Q., Wang, X., Chen, Y., Li, D., Li, L., . . . Chen, H. (2020). The anhedonia is differently modulated by structural covariance network of NAc in bipolar disorder and major depressive disorder. *Progress in Neuro-Psychopharmacology & Biological Psychiatry, 99*, 109865. doi:10.1016/j.pnpbp.2020.109865

Harenski, C. L., Harenski, K. A., Calhoun, V. D., & Kiehl, K. A. (2020). Source-based morphometry reveals gray matter differences related to suicidal behavior in criminal offenders. *Brain Imaging and Behavior 14*(1), 1-9. doi:10.1007/s11682-018-9957-2

Jahn, A., Nee, D. E., Alexander, W. H., & Brown, J. W. (2016). Distinct regions within medial prefrontal cortex process pain and cognition. *Journal of Neuroscience, 36*(49), 12385-12392. doi:10.1523/JNEUROSCI.2180-16.2016

Kaiser, R. H., Andrews-Hanna, J. R., Wager, T. D., & Pizzagalli, D. A. (2015). Large-Scale Network Dysfunction in Major Depressive Disorder: A Meta-analysis of Resting-State Functional Connectivity. *JAMA Psychiatry, 72*(6), 603-611. doi:10.1001/jamapsychiatry.2015.0071

Kakeda, S., Watanabe, K., Nguyen, H., Katsuki, A., Sugimoto, K., Igata, N., . . . Korogi, Y. (2020). An independent component analysis reveals brain structural networks related to TNF-alpha in drug-naive, first-episode major depressive disorder: a source-based morphometric study. *Translational Psychiatry, 10*(1), 187. doi:10.1038/s41398-020-00873-8

Kandilarova, S., Stoyanov, D., Sirakov, N., Maes, M., & Specht, K. (2019). Reduced grey matter volume in frontal and temporal areas in depression: contributions from voxel-based morphometry study. *Acta Neuropsychiatrica, 31*(5), 252-257. doi:10.1017/neu.2019.20

Kessler, R. C., Angermeyer, M., Anthony, J. C., R, D. E. G., Demyttenaere, K., Gasquet, I., . . . Ustun, T. B. (2007). Lifetime prevalence and age-of-onset distributions of mental disorders in the World Health Organization's World Mental Health Survey Initiative. *World Psychiatry, 6*(3), 168-176.

Kocsis, K., Holczer, A., Kazinczi, C., Boross, K., Horvath, R., Nemeth, L. V., . . . Must, A. (2021). Voxel-based asymmetry of the regional gray matter over the inferior temporal gyrus correlates with depressive symptoms in medicated patients with major depressive disorder. *Psychiatry Research: Neuroimaging, 317*, 111378. doi:10.1016/j.pscychresns.2021.111378

Kunst, J., Marecek, R., Klobusiakova, P., Balazova, Z., Anderkova, L., Nemcova-Elfmarkova, N., & Rektorova, I. (2019). Patterns of Grey Matter Atrophy at Different Stages of Parkinson's and Alzheimer's Diseases and Relation to Cognition. *Brain Topography 32*(1), 142-160. doi:10.1007/s10548-018-0675-2

Li, B. J., Friston, K., Mody, M., Wang, H. N., Lu, H. B., & Hu, D. W. (2018). A brain network model for depression: From symptom understanding to disease intervention. *CNS Neuroscience & Therapeutics, 24*(11), 1004-1019. doi:10.1111/cns.12998

Li, J., Seidlitz, J., Suckling, J., Fan, F., Ji, G. J., Meng, Y., . . . Liao, W. (2021). Cortical structural differences in major depressive disorder correlate with cell type-specific transcriptional signatures. *Nature Communications, 12*(1), 1647. doi:10.1038/s41467-021-21943-5

Li, Q., Zhao, Y. J., Chen, Z. Q., Long, J. Y., Dai, J., Huang, X. Q., . . . Gong, Q. Y. (2020). Meta-analysis of cortical thickness abnormalities in medication-free patients with major depressive disorder. *Neuropsychopharmacology, 45*(4), 703-712. doi:10.1038/s41386-019-0563-9

Menon, V. (2011). Large-scale brain networks and psychopathology: a unifying triple network model. *Trends in Cognitive Sciences, 15*(10), 483-506. doi:10.1016/j.tics.2011.08.003

Miller, E. K. (2000). The prefrontal cortex and cognitive control. *Nature Review Neuroscience, 1*(1), 59-65. doi:10.1038/35036228

Murty, V. P., Ritchey, M., Adcock, R. A., & LaBar, K. S. (2010). fMRI studies of successful emotional memory encoding: A quantitative meta-analysis. *Neuropsychologia, 48*(12), 3459-3469. doi:10.1016/j.neuropsychologia.2010.07.030

Nguyen, L., Kakeda, S., Watanabe, K., Katsuki, A., Sugimoto, K., Igata, N., . . . Yoshimura, R. (2020). Brain structural network alterations related to serum cortisol levels in drug-naive, first-episode major depressive disorder patients: a source-based morphometric study. *Scientific Reports, 10*(1), 22096. doi:10.1038/s41598-020-79220-2

Nobbelin, L., Bogren, M., Mattisson, C., & Bradvik, L. (2018). Risk factors for recurrence in depression in the Lundby population, 1947-1997. *Journal of Affective Disorders, 228*, 125-131. doi:10.1016/j.jad.2017.11.038

Okamoto, N., Watanabe, K., Ngyuyen, L., Ikenouchi, A., Kishi, T., Iwata, N., . . . Yoshimura, R. (2020). Association of Serum Kynurenine Levels and Neural Networks in Patients with First-Episode, Drug-Naive Major Depression: A Source-Based Morphometry Study. *Neuropsychiatric Disease and Treatment, 16*, 2569-2577. doi:10.2147/NDT.S279622

Pappaianni, E., Siugzdaite, R., Vettori, S., Venuti, P., Job, R., & Grecucci, A. (2018). Three shades of grey: detecting brain abnormalities in children with autism using source-, voxel- and surface-based morphometry. *European Journal of Neuroscience, 47*(6), 690-700. doi:10.1111/ejn.13704

Paquola, C., Bennett, M. R., & Lagopoulos, J. (2018). Structural and Functional Connectivity Underlying Gray Matter Covariance: Impact of Developmental Insult. *Brain Connectivity, 8*(5), 299-310. doi:10.1089/brain.2018.0584

Pierce, J. E., & Peron, J. (2020). The basal ganglia and the cerebellum in human emotion. *Social Cognitive and Affective Neuroscience, 15*(5), 599-613. doi:10.1093/scan/nsaa076

Rice, F., Riglin, L., Lomax, T., Souter, E., Potter, R., Smith, D. J., . . . Thapar, A. (2019). Adolescent and adult differences in major depression symptom profiles. *Journal of Affective Disorders, 243*, 175-181. doi:10.1016/j.jad.2018.09.015

Rohr, C. S., Vinette, S. A., Parsons, K. A. L., Cho, I. Y. K., Dimond, D., Benischek, A., . . . Bray, S. (2017). Functional Connectivity of the Dorsal Attention Network Predicts Selective Attention in 4-7 year-old Girls. *Cerebral Cortex, 27*(9), 4350-4360. doi:10.1093/cercor/bhw236

Rolls, E. T., Cheng, W., Du, J., Wei, D., Qiu, J., Dai, D., . . . Feng, J. (2020). Functional connectivity of the right inferior frontal gyrus and orbitofrontal cortex in depression. *Social Cognitive and Affective Neuroscience, 15*(1), 75-86. doi:10.1093/scan/nsaa014

Scangos, K. W., Khambhati, A. N., Daly, P. M., Makhoul, G. S., Sugrue, L. P., Zamanian, H., . . . Chang, E. F. (2021). Closed-loop neuromodulation in an individual with treatment-resistant depression. *Nature Medicine, 27*(10), 1696-1700. doi:10.1038/s41591-021-01480-w

Schmaal, L., Hibar, D. P., Samann, P. G., Hall, G. B., Baune, B. T., Jahanshad, N., . . . Veltman, D. J. (2017). Cortical abnormalities in adults and adolescents with major depression based on brain scans from 20 cohorts worldwide in the ENIGMA Major Depressive Disorder

Working Group. *Molecular Psychiatry, 22*(6), 900-909. doi:10.1038/mp.2016.60

Schmaal, L., Pozzi, E., T, C. H., van Velzen, L. S., Veer, I. M., Opel, N., . . . Veltman, D. J. (2020). ENIGMA MDD: seven years of global neuroimaging studies of major depression through worldwide data sharing. *Translational Psychiatry, 10*(1), 172. doi:10.1038/s41398-020-0842-6

Schmaal, L., Veltman, D. J., van Erp, T. G., Samann, P. G., Frodl, T., Jahanshad, N., . . . Hibar, D. P. (2016). Subcortical brain alterations in major depressive disorder: findings from the ENIGMA Major Depressive Disorder working group. *Molecular Psychiatry, 21*(6), 806-812. doi:10.1038/mp.2015.69

Schneier, F. R., Slifstein, M., Whitton, A. E., Pizzagalli, D. A., Reinen, J., McGrath, P. J., . . . Abi-Dargham, A. (2018). Dopamine Release in Antidepressant-Naive Major Depressive Disorder: A Multimodal [11C]-(+)-PHNO Positron Emission Tomography and Functional Magnetic Resonance Imaging Study. *Biological Psychiatry, 84*(8), 563-573. doi:10.1016/j.biopsych.2018.05.014

Schultz, W., Tremblay, L., & Hollerman, J. R. (2000). Reward processing in primate orbitofrontal cortex and basal ganglia. *Cerebral Cortex, 10*(3), 272-284. doi:10.1093/cercor/10.3.272

Serra-Blasco, M., Radua, J., Soriano-Mas, C., Gomez-Benlloch, A., Porta-Casteras, D., Carulla-Roig, M., . . . Cardoner, N. (2021). Structural brain correlates in major depression, anxiety disorders and post-traumatic stress disorder: A voxel-based morphometry meta-analysis. *Neuroscience & Biobehavioral Reviews, 129*, 269-281. doi:10.1016/j.neubiorev.2021.07.002

Shen, X., MacSweeney, N., Chan, S. W. Y., Barbu, M. C., Adams, M. J., Lawrie, S. M., . . . Whalley, H. C. (2021). Brain structural associations with depression in a large early adolescent sample (the ABCD study(R)). *EClinicalMedicine, 42*, 101204. doi:10.1016/j.eclinm.2021.101204

Singh, A., Arya, A., Agarwal, V., Shree, R., & Kumar, U. (2021). Grey and white matter alteration in euthymic children with bipolar disorder: a combined source-based morphometry (SBM) and voxel-based morphometry (VBM) study. *Brain Imaging and Behavior*. doi:10.1007/s11682-021-00473-0

Sokolov, A. A., Miall, R. C., & Ivry, R. B. (2017). The Cerebellum: Adaptive Prediction for Movement and Cognition. *Trends in Cognitive Sciences, 21*(5), 313-332. doi:10.1016/j.tics.2017.02.005

Spreng, R. N., & Turner, G. R. (2013). Structural covariance of the default network in healthy and pathological aging. *Journal of Neuroscience, 33*(38), 15226-15234. doi:10.1523/JNEUROSCI.2261-13.2013

Suarez, L. E., Markello, R. D., Betzel, R. F., & Misic, B. (2020). Linking Structure and Function in Macroscale Brain Networks. *Trends in Cognitive Sciences, 24*(4), 302-315. doi:10.1016/j.tics.2020.01.008

Sullivan, C. R. P., Olsen, S., & Widge, A. S. (2021). Deep brain stimulation for psychiatric disorders: From focal brain targets to cognitive networks. *Neuroimage, 225*, 117515. doi:10.1016/j.neuroimage.2020.117515

Wang, L., LaBar, K. S., Smoski, M., Rosenthal, M. Z., Dolcos, F., Lynch, T. R., . . . McCarthy, G. (2008). Prefrontal mechanisms for executive control over emotional distraction are altered in major depression. *Psychiatry Research, 163*(2), 143-155. doi:10.1016/j.pscychresns.2007.10.004

Wang, T., Wang, K., Qu, H., Zhou, J., Li, Q., Deng, Z., . . . Xie, P. (2016). Disorganized cortical thickness covariance network in major depressive disorder implicated by aberrant hubs in large-scale networks. *Scientific Reports, 6*, 27964. doi:10.1038/srep27964

Watanabe, K., Kakeda, S., Katsuki, A., Ueda, I., Ikenouchi, A., Yoshimura, R., & Korogi, Y. (2020). Whole-brain structural covariance network abnormality in first-episode and drug-naive major depressive disorder. *Psychiatry Research: Neuroimaging, 300*, 111083. doi:10.1016/j.pscychresns.2020.111083

Wolf, R. C., Nolte, H. M., Hirjak, D., Hofer, S., Seidl, U., Depping, M. S., . . . Thomann, P. A. (2016). Structural network changes in patients with major depression and schizophrenia treated with electroconvulsive therapy. *European Neuropsychopharmacology, 26*(9), 1465-1474. doi:10.1016/j.euroneuro.2016.06.008

Wu, H. W., Sun, H., Wang, C., Yu, L., Li, Y. L., Peng, H. J., . . . Wang, J. J. (2017). Abnormalities in the structural covariance of emotion regulation networks in major depressive disorder. *Journal of Psychiatric Research, 84*, 237-242. doi:10.1016/j.jpsychires.2016.10.001

Xu, L., Groth, K. M., Pearlson, G., Schretlen, D. J., & Calhoun, V. D. (2009). Source-based morphometry: the use of independent component analysis to identify gray matter differences with application to schizophrenia. *Human Brain Mapping, 30*(3), 711-724. doi:10.1002/hbm.20540

Yan, C. G., Chen, X., Li, L., Castellanos, F. X., Bai, T. J., Bo, Q. J., . . . Zang, Y. F. (2019). Reduced default mode network functional connectivity in patients with recurrent major depressive disorder. *Proceedings of the National Academy of Sciences of the United States of America, 116*(18), 9078-9083. doi:10.1073/pnas.1900390116

Yan, C. G., & Zang, Y. F. (2010). DPARSF: A MATLAB Toolbox for "Pipeline" Data Analysis of Resting-State fMRI. *Frontiers in Systems Neuroscience, 4*, 13. doi:10.3389/fnsys.2010.00013

Yang, X., Kumar, P., Nickerson, L. D., Du, Y., Wang, M., Chen, Y., . . . Ma, X. (2021). Identifying subgroups of major depressive disorder using brain structural covariance networks and mapping of associated clinical and cognitive variables. *Biological Psychiatry Global Open Science, 1*(2), 135-145.

Yoon, Y. B., Shin, W. G., Lee, T. Y., Hur, J. W., Cho, K. I. K., Sohn, W. S., . . . Kwon, J. S. (2017). Brain Structural Networks Associated with Intelligence and Visuomotor Ability. *Scientific Reports, 7*(1), 2177. doi:10.1038/s41598-017-02304-z

Zhou, H. X., Chen, X., Shen, Y. Q., Li, L., Chen, N. X., Zhu, Z. C., . . . Yan, C. G. (2020). Rumination and the default mode network: Meta-analysis of brain imaging studies and implications for depression. *Neuroimage, 206*, 116287. doi:10.1016/j.neuroimage.2019.116287

Zielinski, B. A., Gennatas, E. D., Zhou, J., & Seeley, W. W. (2010). Network-level structural covariance in the developing brain. *Proceedings of the National Academy of Sciences of the United States of America, 107*(42), 18191-18196. doi:10.1073/pnas.1003109107

## Figures and Tables

Figure 1. Decreased grey matter volume in patients with major depressive disorder compared to healthy controls. Results were shown with a voxel-level threshold at $p<0.001$ and a cluster-level threshold at $p < 0.05$ (FWE corrected). Sagittal and axial slices were shown with the ICBM52 MNI brain template.

Figure 2. Abnormal structural covariance networks in MDD patients vs. healthy controls, and FEDN MDD patients vs. recurrent patients. (A) The loading coefficients of the MDD patients in the prefrontal network were significantly lower than those of the healthy participants. (B) Compared to FEDN MDD patients, recurrent MDD patients showed lower loading coefficients in these five structural covariance networks.

Table 1. Sample characteristics of all depressive patients and healthy controls, and subgroup of patients

Table 2. Grey matter volume differences between 1082 major depressive disorder patients and 990 healthy controls

Table 3. Differences in structural covariance networks between all MDD patients vs. healthy controls, and FEDN patients vs. recurrent patients

Table 4. Location of structural covariance networks for which significant differences were observed in comparisons between MDD patients vs. healthy controls, FEDN MDD patients vs. healthy controls, recurrent MDD patients vs. healthy controls, and FEDN patients vs. recurrent MDD patients.

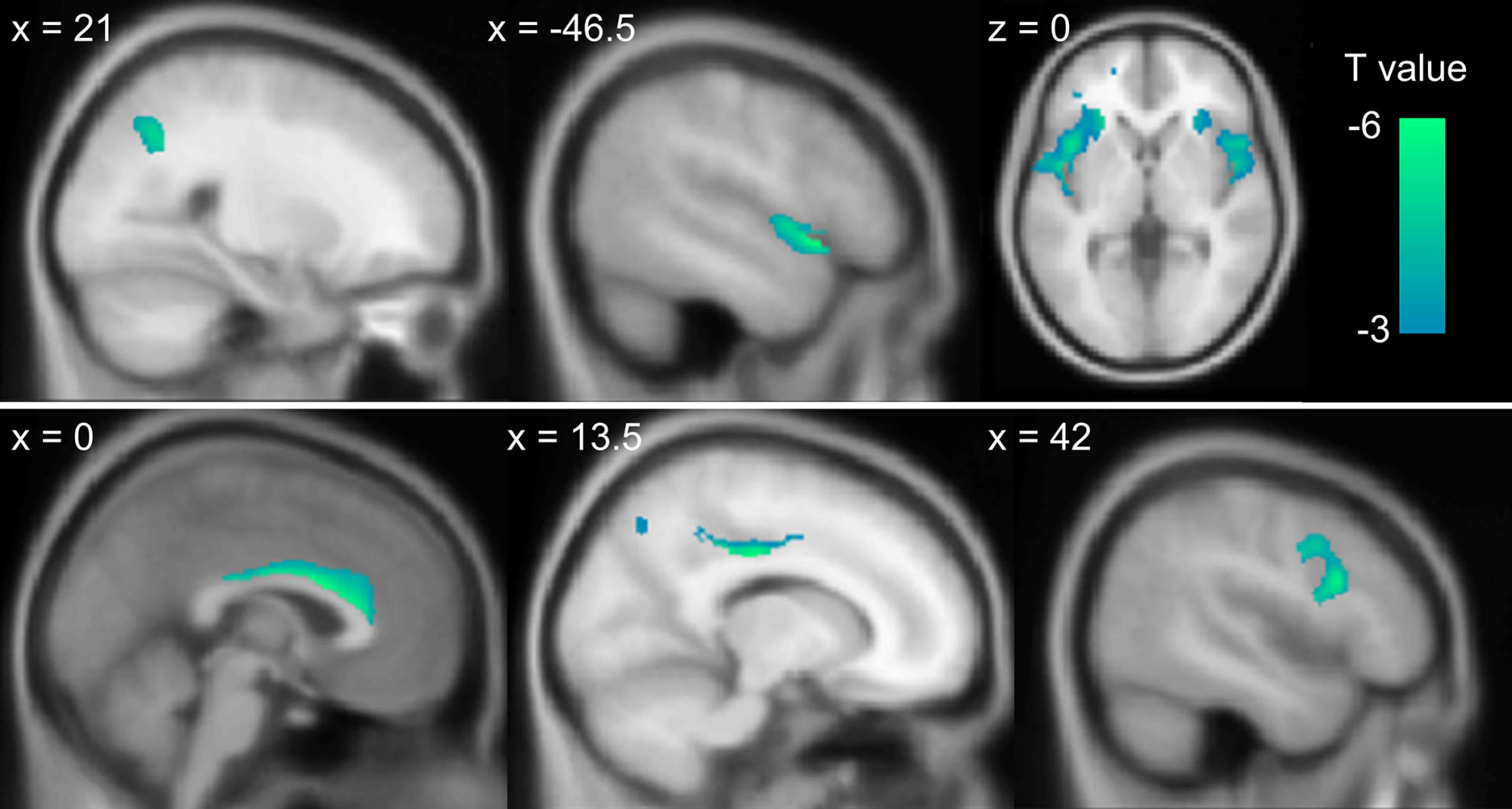
x = 21
x = -46.5
z = 0
T value
-6
-3
x = 0
x = 13.5
x = 42

A. MDD patients lower than healthy controls

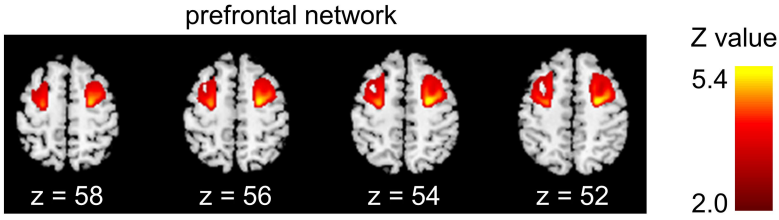


B. FEDN MDD patients higher than recurrent MDD patients

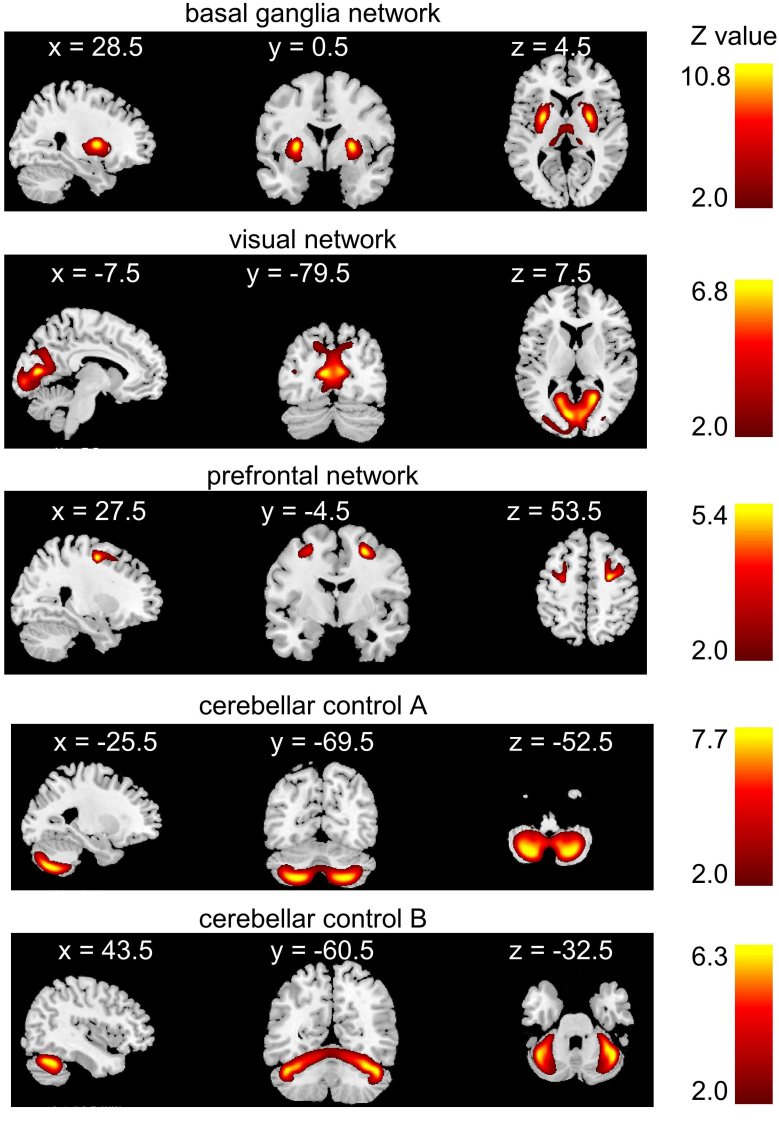

Table 1. Sample characteristics of all depressive patients and healthy controls, and subgroup of patients

| Variables | MDD patients | Healthy controls | p | FEDN patients | Recurrent patients | p |
|---|---|---|---|---|---|---|
| Sample size | N = 1082 | N = 990 | | N = 430 | N = 207 | |
| Gender (male, N(%)) | 404(37.34) | 410(41.41) | 0.058 | 145(33.72) | 80(38.65) | 0.223 |
| Age (years) | 37.23(14.20) | 37.45(15.67) | 0.732 | 35.85(12.00) | 37.67(13.36) | 0.085 |
| Education (years) | 11.63(3.71) | 13.25(3.73) | <0.001 | 11.33(3.75) | 10.98(3.65) | 0.266 |
| Illness duration (months) | 38.34(61.51) | - | - | 21.60 (37.69) | 94.67 (87.04) | <0.001 |
| HAMD | 20.75(7.48) | - | - | 21.44(5.87) | 19.10 (7.85) | <0.001 |
| HAMA | 19.09 (9.04) | - | - | 21.52 (8.75) | 17.57(8.65) | <0.001 |

Abbreviation: MDD, major depressive disorder; FEDN, first episode drug naïve; HAMD, Hamilton depression rating scale; HAMA, Hamilton anxiety scale. Group differences were compared using two sample t-tests or chi-square test (gender only).

Table 2. Grey matter volume differences between 1082 patients with major depressive disorder and 990 healthy controls

| Brain regions | Hemisphere | Brodmann area | Cluster size | MNI coordinates | | | t-value |
|---|---|---|---|---|---|---|---|
| | | | | x | y | z | |
| Superior temporal cortex | left | BA38 | 293 | -46.5 | 10.5 | -9 | -6.90 |
| Superior temporal cortex | right | BA22 | 141 | 49.5 | 13.5 | -4.5 | -7.02 |
| Dorsal anterior cingulate cortex | / | BA24/33 | 435 | 0 | 9 | 24 | -6.25 |
| Middle cingulate cortex | right | BA24 | 169 | 13.5 | -21 | 36 | -6.28 |
| Inferior frontal cortex | right | BA46 | 134 | 42 | 13.5 | 21 | -6.85 |
| Precuneus cortex | right | BA7 | 100 | 21 | -61.5 | 42 | -5.90 |

Note: These results were corrected with a voxel-level threshold of $p<0.001$ and a cluster-level threshold of $p < 0.05$ (FWE corrected).

Table 3. Differences in structural covariance networks between all MDD patients vs. healthy controls, and FEDN patients vs. recurrent patients

| | | | | | |
|---|---|---|---|---|---|
| MDD group (n = 1082) vs. HC group (n = 990) | | | | | |
| Name of ICs | MDD group | Control group | Difference | F | $p_{corrected}$ |
| prefrontal network | -0.08 (0.98) | 0.08 (1.02) | -0.16 | 13.10 | < 0.01 |
| FEDN MDD group (n = 430) vs. HC group (n = 990) | | | | | |
| Name of ICs | FEDN MDD group | Control group | Difference | F | $p_{corrected}$ |
| cerebellar control A | 0.21(0.66) | 0.01(1.03) | 0.20 | 13.00 | < 0.01 |
| Superior temporal network | -0.20(0.96) | 0.04 (1.03) | -0.24 | 17.40 | < 0.01 |
| Recurrent MDD group (n = 207) vs. HC group (n = 990) | | | | | |
| Name of ICs | Recurrent MDD group | Control group | Difference | F | $p_{corrected}$ |
| cerebellar control A | -0.22(0.99) | 0.01(1.03) | -0.23 | 8.75 | 0.05 |
| cerebellar control B | -0.21 (1.05) | 0.01 (1.02) | -0.23 | 8.35 | 0.05 |
| basal ganglia network | -0.88(1.17) | 0.003 (1.00) | -0.88 | 124.34 | < 0.001 |
| temporal network | -0.33 (0.95) | 0.04 (1.03) | -0.38 | 23.55 | < 0.001 |
| prefrontal network | -0.17(1.10) | 0.08 (1.02) | -0.25 | 9.90 | <0.05 |
| superior temporal network | 0.29(0.95) | 0.04(1.02) | 0.25 | 10.52 | <0.05 |
| visual network | -0.27(0.94) | -0.014 (1.00) | -0.25 | 11.14 | <0.05 |
| FEDN MDD group (n = 430) vs. Recurrent MDD group (n = 207) | | | | | |
| Name of ICs | FEDN MDD group | Recurrent MDD group | Difference | F | $p_{corrected}$ |
| cerebellar control A | 0.21(0.66) | -0.22 (0.99) | 0.43 | 43.01 | < 0.001 |
| cerebellar control B | 0.14 (0.93) | -0.21 (1.05) | 0.36 | 18.98 | < 0.001 |
| basal ganglia network | -0.07(0.75) | -0.88(1.17) | 0.81 | 109.99 | < 0.001 |
| prefrontal network | 0.08(0.99) | -0.17(1.10) | 0.24 | 7.75 | 0.07* |
| visual network | 0.08(0.98) | -0.27(0.94) | 0.35 | 72.76 | < 0.001 |

Abbreviation: FEDN, first episode drug naïve; MDD, major depressive disorder; HC, healthy controls. The z-scores (mean (standard deviation)) of structural covariance networks were shown for each group. The p values were corrected using Bonferroni correction at $p < 0.05$.

Table 4. Location of structural covariance networks for which significant differences were observed in comparisons between MDD patients vs. healthy controls, FEDN MDD patients vs. healthy controls, recurrent MDD patients vs. healthy controls, and FEDN patients vs. recurrent MDD patients.

| Anatomical regions | Brodmann Area | Volume(cc) Left/right | Maximum z value for left/right hemisphere (MNI coordinates x, y, z) |
|---|---|---|---|
| **Prefrontal network [2,3]** | | | |
| Middle Frontal Gyrus | 6, 8, 9, 10, 46 | 9.9/10.8 | 4.1 (-25, -3, 50)/4.9 (27, -2, 50) |
| Superior Frontal Gyrus | 6, 8, 9, 10 | 2.1/2.6 | 3.1 (-24, 11, 48)/3.4 (25, 10, 49) |
| Inferior Frontal Gyrus | 9, 46 | 1.0/0.6 | 3.1 (-45, 7, 33)/3.5 (42, 9, 33) |
| Precentral Gyrus | 6, 9 | 1.0/0.7 | 4.1 (-39, 5, 37)/3.8 (40, 8, 37) |
| **Basal ganglia network [2,3]** | | | |
| Lentiform Nucleus | / | 4.8/4.0 | 9.9 (-27, 0, 4)/9.8 (28, 0, 4) |
| Extra-Nuclear | 13 | 5.1/4.9 | 8.0 (-28, 3, 7)/7.8 (31, 3, 3) |
| Thalamus | / | 2.9/2.9 | 4.4 (-4, -13, 6)/4.6 (6, -11, 6) |
| Insula | 13, 47 | 1.7/2.0 | 4.4 (-33, 9, -2)/3.9 (36, -2, -2) |
| **Visual network [2,3]** | | | |
| Cuneus | 7, 17, 18, 19, 23, 30 | 12.5/11.5 | 6.3 (-9, -75, 11)/6.2 (12, -71, 13) |
| Middle Occipital Gyrus | 18, 19, 37 | 4.7/2.1 | 4.4 (-27, -87, 7)/3.1 (31, -81, 10) |
| Posterior Cingulate Cortex | 23, 30, 31 | 3.3/3.9 | 5.8 (-18, -61, 10)/6.3 (21, -58, 10) |
| Precuneus | 7, 19, 23, 31 | 5.1/5.4 | 5.7 (-15, -60, 22)/5.1 (16, -61, 29) |
| Lingual Gyrus | 17, 18, 19 | 5.8/5.4 | 5.3 (-9, -93, 1)/4.9 (3, -77, 5) |
| **Superior temporal network [2]** | | | |
| Superior Temporal Gyrus | 13, 21, 22, 41, 42 | 7.0/2.9 | 9.5 (-42, -30, 14)/5.7 (49, -25, 16) |
| Insula | 13, 40, 41 | 6.5/6.4 | 8.1 (-39, -27, 14)/7.2 (43, -25, 16) |
| Inferior Parietal Lobule | 40 | 3.6/2.5 | 5.6 (-53, -37, 23)/5.3 (46, -28, 22) |
| **Temporal network [1,2]** | | | |
| Inferior Temporal Gyrus | 19, 20, 21, 37 | 5.1/6.0 | 5.4 (-59, -26, -20)/5.5 (59, -26, -21) |
| Middle Temporal Gyrus | 20, 21, 22, 37, 38 | 11.6/12.0 | 4.9 (-61, -34, -12)/5.1 (64, -33, -12) |
| Fusiform Gyrus | 20, 36, 37 | 2.0/1.6 | 4.6 (-59, -17, -23)/5.0 (59, -19, -24) |
| **Cerebellar network A [1,2,3]** | | | |
| Inferior Semi-Lunar Lobule | / | 6.1/6.1 | 7.1 (-27, -69, -41)/7.1 (27, -69, -41) |
| Cerebellar Tonsil | / | 5.5/4.9 | 6.5 (-28, -59, -42)/6.5 (30, -60, -42) |
| Pyramis (Cerebellum) | / | 3.4/3.8 | 5.9 (-31, -75, -34)/6.0 (16, -79, -34) |
| Uvula (Cerebellum) | / | 2.3/2.3 | 5.5 (-15, -75, -34)/5.3 (12, -79, -33) |
| **Cerebellar network B [2,3]** | | | |
| Tuber (Cerebellum) | / | 2.8/2.9 | 5.7 (-42, -58, -25)/5.9 (43, -60, -25) |
| Culmen (Cerebellum) | / | 11.1/10.9 | 5.4 (-40, -54, -25)/5.8 (36, -55, -22) |
| Declive (Cerebellum) | / | 10.8/10.2 | 5.4 (-39, -65, -22)/5.8 (34, -59, -21) |
| Uvula (Cerebellum) | / | 1.6/1.3 | 4.6 (-36, -64, -25)/4.9 (34, -62, -23) |

Note: [1] indicates significant differences between FEDN MDD patients vs. healthy controls; [2] indicates significant differences between recurrent MDD patients vs. healthy controls; [3] indicates significant differences between FEDN MDD patients vs. recurrent MDD patients. The volume of voxels in each area is provided in cubic centimeters (cc).